Dressing of driven colloidal particles in a subcritical liquid suspension

J. Chakrabarti[1,a)] and H. Löwen[2,b)]

[1]*Department of Chemical, Biological and Macromolecular Sciences, S. N. Bose National Centre for Basic Sciences, Block-JD, Sector-III, Salt Lake, Calcutta 700 098, India*
[2]*Institut für Theoretische Physik, Heinrich-Heine Universität, Universitätsstrasse 1, 40225 Düsseldorf, Germany*

At equilibrium, colloidal particles in a subcritical liquid suspension are surrounded by a drying layer if the colloid has solvophobic interaction. Using Brownian dynamics computer simulations, we investigate the nonequilibrium response of this layer to a strong external driving force. We find that the driven colloidal particle dresses itself with more particles than in the equilibrium drying layer. The effective interaction between two such dressed particles exhibits a deep drive-induced attraction due to a stretched joint gas bubble. © *2008 American Institute of Physics.*
[DOI: 10.1063/1.2985830]

I. INTRODUCTION

Micro- and nanoparticles, which are exposed to a surrounding medium that is close to a bulk phase transition can be surrounded by a wetting or drying layer depending on their interaction with the medium particles. While most of the equilibrium properties of wetting and drying layers around nanoparticles are well known by now (see, e.g., Refs. 1 and 2), their nonequilibrium properties are far from being understood. In many applications, however, the nonequilibrium response of particles driven through a subcritical medium is crucial: In granular matter, for example, the dynamical properties[3] and the clustering[4] of wet sand are governed by the motion of the capillary bridges between the particles. Colloidal particles in a subcritical solvent lead to an interesting aggregation behavior[5,6] steered by a collective wetting layer. In the area of liquid-liquid chromatography,[7] a relative motion is created between the dispersed and the dispersing media to separate out the dispersed particles. In general, near-critical solvents gain more and more importance in industrial separation techniques.[8] Last but not the least, nano-sized proteins with a hydrophobic surface[9] are surrounded by a cavity depleted from water[10] and exposed to strong electric driving fields in electrophoretic measurements.

In a previous study,[11] we considered a model system in two dimensions (2D) to show that two dry spheres in equilibrium in a subcritical liquid exhibit a long-ranged attractive effective interaction.[12–16] Here we investigate how a strong external force affects the dry layer around the driven particles within the simple model system in 2D as in Ref. 11. The big particle is driven in a liquid suspension of smaller particles below their liquid-gas coexistence. Our motivation to do so is threefold: First, the trends obtained from our model should be transferable in general and applicable to quite different fields and setups as outlined above. Second, our model is realized by confined two-dimensional colloidal

suspensions, which can be exposed to controlled driving fields and can be watched by video microscopy in real space.[17] Third, we want to study the combined effect of drive and fluctuations; therefore, we adopt a "microscopic," i.e., particle resolved, view of the wetting layers such that fluctuations are contained in our investigations. We use Brownian dynamics (BD) computer simulations to explore the nonequilibrium response of the drying layer around the colloids to a strong drive where the drift motion of the driven colloidal particles is so fast that the smaller particles cannot follow[18] the big particle instantaneously. This is complementary to the widely studied adiabatic approximation where the motion of the big particles is so slow that the small particles follow almost instantaneously and an equilibrium picture applies. As a result, we find a *dressing* effect in the drying layer around a single driven particle. In detail, a drying layer is significantly compressed upon the drive through a bulk liquid. The effective drag force, which opposes the motion of a driven big particle, exhibits an initial elastic regime, followed by a viscosity dominated regime. There is a deep drive-induced attraction due to a stretched joint gas bubble surrounding the big particles.

The outline of the paper is as follows. We detail the model and the simulation techniques in Sec. II. The detailed results on the small particle distribution around a big particle are given in Sec. III. We account for the long time distribution of the small particles around the driven big particle by a simple hydrodynamic instability theory. The effective interaction between two driven big particles is illustrated in Sec. IV. Then the importance of the hydrodynamic interactions between the particles in our model has been discussed in Sec. V before we conclude the paper in Sec. VI.

II. SIMULATION DETAILS

We model the interaction between two small particles at separation r by a Lennard-Jones (LJ) pair potential, $V_{LJ}(r) = 4\epsilon[(\sigma/r)^{12} - (\sigma/r)^6]$ with interaction parameters ϵ and σ at a subcritical temperature ($k_B T / \epsilon = 0.45$) and chemical poten-

tial $\mu/k_BT(=-3.7)$ above that of the gas-liquid coexistence as in Ref. 11. The stable bulk phase of the small particles is liquid for chemical potential above the coexistence. The big particles have vanishingly small area fraction. A big particle surface, having a purely repulsive solvophobic interaction, $V_{bs}(|\vec{r}-\vec{R}|)=4\epsilon_{bs}(d/|\vec{r}-\vec{R}|)$,[12] becomes dry by the metastable gas. We take the big-small interaction energy parameter, $\epsilon_{bs}/\epsilon=5.0$ and the hard-core size of the big particle, $d/\sigma=5.0$. The particles are taken in a box of size, $L=50\sigma$ with the periodic boundary conditions.

For fixed prescribed positions $\{\vec{R}_\alpha\}$ of the big particles, an equilibrated grand canonical Monte Carlo configuration of the small particles is picked up.[19] The drive is then instantaneously applied on the big particles at time $t=0$. The positions of the big and small particles are now updated by the overdamped BD.[19] The position of the ith small particle is shifted by $\gamma_s\delta\vec{r}_i=-\delta t\partial_{\vec{r}_i}[\Sigma_j' V_{LJ}(|\vec{r}_i-\vec{r}_j|)+\Sigma_\alpha V_{bs}(|\vec{r}_i-\vec{R}_\alpha|)]+\vec{r}_i^N$. Similarly, the coordinates of the αth big particle are updated by $\gamma_b\delta\vec{R}_\alpha=-\delta t[\partial_{\vec{R}_\alpha}\Sigma_i V_{bs}(|\vec{r}_i-\vec{R}_\alpha|)+\partial_{\vec{R}_\alpha}\Sigma_\beta V_{bb}(|\vec{R}_\alpha-\vec{R}_\beta|)+\vec{F}_\alpha]+\vec{R}_\alpha^N$. Here, the direct big-big interaction, $V_{bb}(|\vec{R}_\alpha-\vec{R}_\beta|)=4\epsilon_{bb}(d/|\vec{R}_\alpha-\vec{R}_\beta|)^{12}$, with $\epsilon_{bb}=\epsilon_{bs}$. $\vec{r}_i^N$ is the random force on a small particle, assumed to be a Gaussian white noise with mean zero and variance $2D_s\delta t$ in each component, where $D_s=k_BT/\gamma_s$. $\vec{R}_\alpha^N$ is the Gaussian white noise for the big particle with mean zero and variance $2k_BT\delta t/\gamma_b$, where $\gamma_b/\gamma_s=5$. Finally, $\vec{F}_\alpha$ is the drive force on the αth big particle. We consider the case in which the magnitude of the driving force is the same for all α. The unit of length is σ and that of time is the diffusion time scale of the small particles, $\tau_s=\sigma^2/D_s$. We use $\delta t/\tau_s=10^{-4}$ such that $\delta t<\tau_b$, τ_b being the time scale set by the drive force on the big particles, given by the $\gamma_b\sigma/F$, with F as the magnitude of the driving force. The time dependence of any quantity of interest has been tracked down up to a late time ($t>\tau_s$) until a big particle covers a distance equal to half of the box length to avoid artifacts due to the periodic boundary conditions. For a given t, the quantities of interest have been averaged over 500 different realizations of the noise and the initial configurations of the small particles. In our simulations, we have ignored hydrodynamic interactions mediated by the solvent flow. In Sec. V we discuss several setup where this assumption is justified.

III. SINGLE PARTICLE RESULTS

We first study the case of a single big particle driven parallel to the x-axis, as shown in inset I of Fig. 1 with a large reduced drive force (or Peclet number) of $f=F\sigma/k_BT=50$. ϕ measures polar angle with respect to the x-axis. The drive force corresponds to $\phi=\pi$. At equilibrium, the big particle is surrounded by a gas bubble of radius $l>d$.[11] Inset I shows a configuration of the small particles around the driven big particle at time $t>\tau_s$. The snapshot shows anisotropic stretching of the gas bubble surrounding the big particle: The big particle pushes the small particles off its trail that leads to the ordering of the small particles transverse to the drive direction. Further, the wake area ($\phi\sim0$) will tend to be populated by the small particles. The steady state flux of the small particles is given by $\rho_L\vec{v}$, where ρ_L is the average
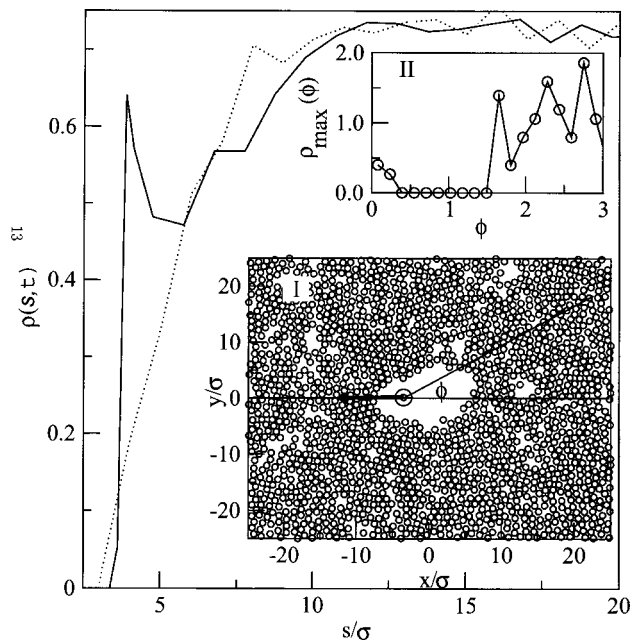

FIG. 1. $\bar{\rho}(s,t)\sigma^2$ plots as a function of s/σ at $t<\tau_s$ (dotted line) and $t>\tau_s$ (solid line) for an initially equilibrated dry sphere driven at $f=50$ in a subcritical liquid bath. Inset I: A snapshot of the small particles along with a big particle (concentric circle) at $t>\tau_s$. The driving force shown by the thick arrows and the angle ϕ indicated. Inset II: The dependence of $\rho_{max}(\phi)$ on ϕ for small particles at the first peak of the solid line.

density of the liquid of small particles and $\vec{v}$ is the velocity of a small particle. In the overdamped limit, $\vec{v}=\vec{F}_s/\gamma_s$, where $\vec{F}_s$ is the force on a small particle. Since $\epsilon_{bs}>\epsilon$, the big-small interaction dominates in $\vec{F}_s$, which implies that the leading contribution to the x-component of the flux has a contribution, proportional to $-f/\gamma_b$, to the wake area.

The response of the small particles to the drive can be characterized by its time dependent density profile $\rho(s,\phi,t)\times(s=|\vec{r}-\vec{R}(t)|)$ around the big particle at $\vec{R}(t)$. Figure 1 shows angle (ϕ) averaged density $\bar{\rho}(s,t)$ of the small particles around the big one. Even though $\bar{\rho}(s,t)$ loses the anisotropy induced by the drive, this illustrates an important effect of the drive. $\bar{\rho}(s,t)$ at $t<\tau_s$ (dotted line) is similar to that in the equilibrium.[11] For $t\simeq\tau_s$, the small particles, forming a gas "bubble" surrounding the big particle, could not follow the big particle. However, at large times, $t>\tau_s$, $\bar{\rho}(s,t)$ (solid line) shows "dressing" of the big particle, namely, the growth of liquid layers of the small particles around the big particle. This modifies the interfacial structure nontrivially, which can be characterized by the quotient $\int_0^{s_{max}}dss\bar{\rho}(s,t>\tau_s)/\int_0^{s_{max}}dss\bar{\rho}(s,t<\tau_s)$, where $s_{max}\simeq7.5$. The quotient of ~2.0 indicates that nearly twice as much as the initial number of particles gather around the big particle in the long time limit. The anisotropy in the small particle distribution at the first peak of the late time $\bar{\rho}(s,t)$, $\rho_{max}(\phi)$ has been shown in inset II of Fig. 1. The $\rho_{max}(\phi)$ plot has multiple peak structure: in addition to the peaks of the distribution in the forward region (0.9π), there are strong peaks around $\phi=0.5\pi$ and 0.7π, nearly transverse to the drive, and as well, some population at $\phi=0$, the wake region. This anisotropy is in

agreement with the picture suggested by the snapshot of inset I. Thus the dressing of the big particle by the small ones in the late time limit is highly anisotropic.

The large time density response of the small particles can be understood from a simple instability analysis[20] of the density modes. The equation of motion for a density modes with wavevector $\vec{q}(=q_x, q_y)$ is given by:[21] $\partial_t \rho(\vec{q}, t)$ $= [-D_0 q^2/s(q)]\rho(\vec{q}, t) - \exp i[\vec{q} \cdot \vec{R}]\Sigma_Q \vec{q} \cdot (\vec{q} - \vec{Q})\widetilde{V}_{bs}(|\vec{q} - \vec{Q}|)$ $\times \rho(\vec{Q}, t)$. The first term describes the small particles correlations, $s(q)$ being the liquid structure factor.[22] The second term describes the scattering of the density mode of wavevector $\vec{q}$ into that of wavevector $\vec{Q}$ by the solute-solvent interaction potential. The phase factor $\exp i(\vec{q} \cdot \vec{R})$ is due to the mobile big particle scatterer. The scattering amplitude $\widetilde{V}_{bs}(|\vec{q} - \vec{Q}|)$ have a peak for elastic scattering, $|\vec{q}| = |\vec{Q}|$, which corresponds to rotating the incident $\vec{q}$, keeping its magnitude fixed. We consequently retain amplitude only at zero wavevector value V_0. In order to eliminate the fast variable $\vec{R}$, we take further time derivative of the density in the equation of motion. In the second order differential equations for the density modes, we approximate $X \sim (f/\gamma)\tau_s$ and $d\vec{X}/dt$ $\sim f/\gamma$ for very strong drive at large times, $t \sim \tau_s$. Retaining only the linear terms in the density modes, the resulting frequency,

$$\omega(q_x, q_y)\tau_s = (1/2)[-D_0 q^2/s(q)] \pm [(-D_s q^2/s(q))^2 - 16V_0 q^2 (q_x v_d \tau_s)^2]^{1/2}.$$

Since $V_0 > 0$ for repulsive solute-solvent interactions, $\omega(q_x, q_y)$ can have a maximum positive for nontrivial $(q_x d \simeq 0.1, q_y d \sim 2\pi)$, indicating an inhomogeneous distribution of the small particles, transverse to the drive.

The effective drag force opposing the motion of a single big particle, $\vec{F}_{bs}(t) = \langle \vec{\nabla}_{\vec{R}} \Sigma_i V_{bs}(|\vec{r}_i(t) - \vec{R}(t)|)\rangle$, $\langle \cdots \rangle$ denoting average over equilibrated initial configurations of the small particles. By symmetry, the y-components of the vectors $\vec{F}_{bs}$ and $\vec{R}(t)$, perpendicular to the drive, vanish and, hence, $\vec{R}(t) = X(t)\vec{e}_x$. We eliminate t from $\vec{F}_{bs}(t)$ and the trajectory of the big particle $X(t)\vec{e}_x$ to obtain the effective drag force on a big particle as a function of distance from the initial equilibrium position, $\vec{F}_{bs}(X)$. The x-component of the effective drag force $F_{bs}(X)$ at $f = 50$ in a subcritical liquid has been shown in Fig. 2 (solid line). A force with a negative sign is taken to be opposite to the drive. $F_{bs}(X)$ is a linear restoring force for small X, showing an elastic regime. The initial elastic regime originates from the unchanged equilibrium small particle distribution for short time. In this static background, the energy of the big particle at $\vec{R}$ is given by $U(\vec{R}) = \int d\vec{r}\rho(|\vec{r} - \vec{R}|)V_{bs}(|\vec{r} - \vec{R}|)]$. Expanding $U(\vec{R})$ in $\vec{R}$, one obtains a linear restoring force $-kX$ with slope given by $k = \frac{1}{2}\int d\vec{\xi}\rho(\xi)d^2 V_{uv}(\xi)/d\xi^2$, where $\rho(\xi)$ is the equilibrium small particle density profile around the big particle. For steep repulsion, the integral is dominated by the interfacial profile and $k \sim 20.0$ in the reduced units, slightly higher than that in the simulated data. Figure 2 shows the theoretical estimate (dashed line) for $F_{bs}(X)$. $F_{bs}(X)$ saturates to $F_{sat} = -40k_B T/\sigma$
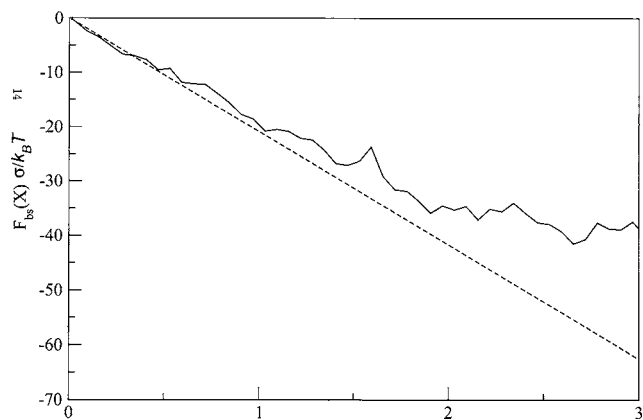

FIG. 2. The x-component of the small particle mediated drag force on a single big dry particle $F_{bs}(X)\sigma/k_B T$ vs its displacement X/σ from the initial equilibrium position, driven at $f = 50$ in a subcritical liquid bath (solid line). The dashed line shows the theoretical estimate for the linear restoring force.

with marked deviation from the linear behavior around $X = X_0 \sim 2.0$, which corresponds to a time $\tau_0 \sim \gamma_b X_0/F_{sat}$ $= \gamma_b/kX_0$. This time is comparable to the diffusive density relaxation time in the surrounding liquid medium, given by $S_{max}\tau_s$, where $S_{max} (=4.0$, typical for a 2D liquid) is the first peak height of the liquid static structure factor.[22] This implies that the onset of F_{sat} is primarily governed by the diffusive motion of the surrounding small particles in the liquid phase.

IV. EFFECTIVE INTERACTION

We finally study the influence of a strong drive on the effective force between a pair of big particles. The particles are initially placed at a separation of 6σ along the x-axis, equilibrated, and then pulled apart $(f = 50)$, as shown in inset I of Fig. 3. The effective force between the two big particles at $\vec{R}_1(t)$ and $\vec{R}_2(t)$ at time t, $\vec{F}^{eff}(t)$
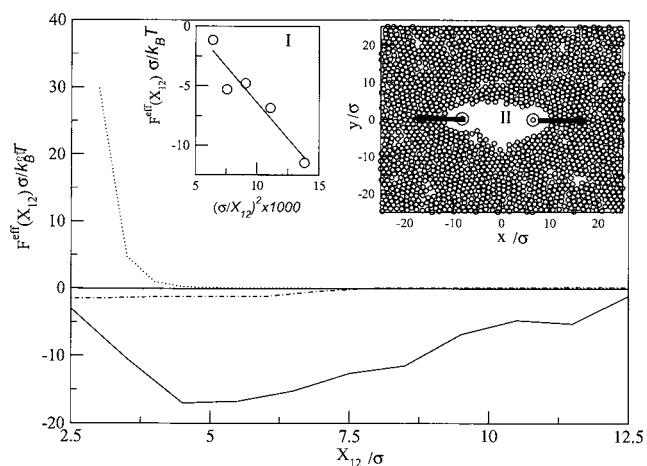

FIG. 3. The x-component of the effective force $F^{eff}(X_{12})\sigma/k_B T$ between a pair of big particles pulled apart from each other at $f = 50$ as a function of the separation X_{12}/σ between them in a subcritical liquid (solid line). The equilibrium case in a subcritical liquid (dot-dashed line) is shown as well for comparison. The dotted line shows the direct repulsion between two big spheres. Inset I: A snapshot at $t/\tau_s = 4.0$ with two big particles pulled out from each other in a subcritical liquid at $f = 50$. The thick arrows show the drive direction. Inset II: The $(\sigma/X_{12})^2$ dependence of $F^{eff}(X_{12})\sigma/k_B T$ for intermediate X_{12}/σ.
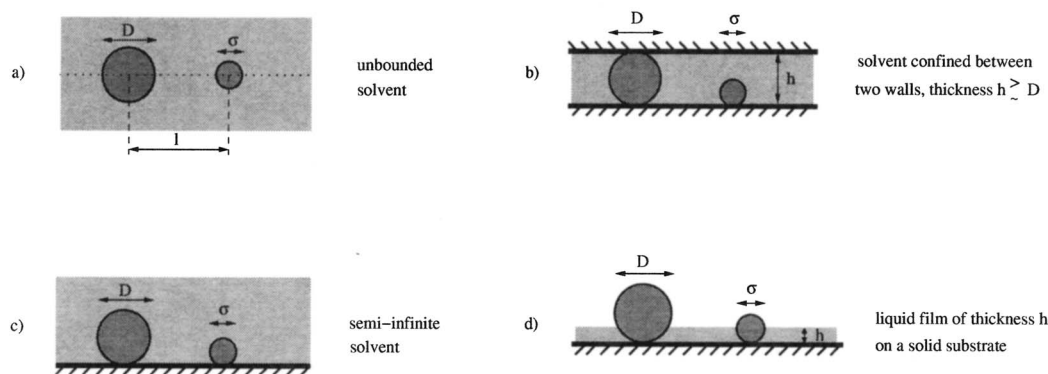
FIG. 4. Sketch of four different setups (a), (b), (c), and (d) for a two-dimensional colloidal mixture in various solvent geometries (side view). One big particle of diameter D and a small particle of diameter σ at a distance ℓ are shown.

$= \langle -[\vec{\nabla}_1 \Sigma_i V_{bs}(|\vec{r}_i(t) - \vec{R}_1(t)|)] \cdot \vec{R}_{12}(t) \rangle$, where $\vec{R}_{12}(t) = \vec{R}_1(t) - \vec{R}_2(t)$ and the gradient operator is over the coordinates of the first big particle. Eliminating t from $\vec{\mathcal{F}}^{\text{eff}}(t)$ and $\vec{R}_{12}(t)$, we obtain $\vec{F}^{\text{eff}}(\vec{R}_{12})$. This facilitates a direct comparison with the equilibrium effective force, which is dynamically valid within the adiabatic approximation.[23] The direct short-ranged repulsive force between two big spheres has also been shown in Fig. 3 by the dotted line. By symmetry, the effective forces on both the solute particles are equal but opposite in sign and the y-component of the effective force vanishes. The x-component of the effective force $F^{\text{eff}}(X_{12})$ is shown as a function of $X_{12} = |(X_2 - X_1) - d|$, after subtracting the single-particle part $F_{bs}(X)$, in Fig. 3 in the reduced units. The non-equilibrium $\vec{F}^{\text{eff}}(X_{12})$ between two big particles driven in a liquid (solid line) shows a deep minimum $F^{\text{eff}}(X_{12})\sigma \simeq -18k_BT$ around $X_{12} \simeq 5.0$. This is to be contrasted to the equilibrium effective force that has a short-ranged attraction (dot-dashed line).[11] $\vec{F}^{\text{eff}}(X_{12})$ has a linear dependence on X_{12} for $X_{12} < 4.0$, corresponding to the elastic response of the small particles. In the diffusion dominated regime, the gas bubble stretches parallel to the drive (inset I of Fig. 3) in such a way that the total area of the bubble remains constant, leading to an effective attractive force between the big particles that goes as $\sim -1/X_{12}^2$ in order to reduce the line tension at the gas-liquid interface. Inset II shows that the $\vec{F}^{\text{eff}}(X_{12})$ data are consistent with this dependence in the intermediate X_{12} regime. Finally the joint bubble breaks and the attraction almost disappears.

V. IMPORTANCE OF HYDRODYNAMIC INTERACTIONS IN OUR MODEL

In the present model, hydrodynamic interactions between the particles mediated by the solvent flow are neglected. In particular, one may worry that a strongly driven big particle generates a hydrodynamic stress acting on the small particles, which will influence, for instance, the wake behind the driven particle. Here we discuss the relevance of such hydrodynamic interactions for various realizations of the two-dimensional colloidal mixture. Four different possible setups (a)–(d) are sketched as side views in Fig. 4, which we discuss one by one. One obvious realization is to

confine all big and small colloidal particles to a two-dimensional plane by an appropriate external field and keep the solvent unbounded both above and below the plane [setup (a)]. Let us estimate the hydrodynamic interactions between the driven big particle and the small particles in the end of the wake assuming a typical central distance of $\ell \approx 10\sigma$ for the latter. In setup (a) the hydrodynamic interactions are dominated by the long-ranged Oseen tensor,[24] which decays as the inverse distance such that their relative importance as compared to the simple Brownian term is given by $3D_H/4\ell$, where D_H is the hydrodynamic diameter of the big particle. If one equates the hydrodynamic diameter with the interaction diameter, $D_H = D$, then this ratio is 0.4, showing that hydrodynamic interactions are not negligible. However, there are two circumstances where the hydrodynamic interactions can be neglected. First, if the big particles are charged and driven by an electric field, the Oseen tensor is exponentially screened and the leading contribution is of the order of $3D_H/4\ell^3\kappa^2$,[25,26] where κ is the inverse Debye–Hückel screening length. Typically, the reduction in $1/\ell^2\kappa^2$ is of two orders of magnitude at a typical salt concentration in the solvent such that the hydrodynamic interactions are irrelevant. Second, the hydrodynamic interactions can be neglected if the hydrodynamic diameter is much smaller than the interaction diameter as is the case for highly charged suspensions, if the interaction is accounted for via the Derjaguin–Landau–Verwey–Overbeek description and the suspensions is close to the secondary minimum.[27]

The second realization [setup (b)], which is frequently used in experiments,[28] is a suspension that is almost completely squeezed between two parallel confining walls. The no-slip boundary conditions at the two walls lead to reduced hydrodynamic interactions and their relative importance is now given by[28,29] D_H^2/ℓ^2, which is of the order of 0.25 when $D_H = D$. The third realization (c) of a semi-infinite solvent above a wall can again be easily realized in experiments.[30] Here, the importance of hydrodynamic interactions is further reduced to $D_H^3/4\ell^3$,[30] which is about 3% when $D_H = D$ such that hydrodynamic interactions can safely be neglected for this setup. Finally, one may consider colloidal particles on a substrate embedded in a liquid film of thickness h (Ref. 17) [setup (d)]. Then the hydrodynamic interactions are of the range of h and can safely be neglected when $h < D$.[31]

To summarize, apart from the case of an unbounded solvent and neutral big particles, hydrodynamic interactions are strongly reduced for a confined solvent, which is the typical experimental realization justifying the model considered in this paper.

VI. CONCLUSION

In conclusion, we show that if big particles are driven so strongly that the small particles cannot follow the instantaneous positions of the big particles, the small particle degrees of freedom decouple from those of the big ones, leading to qualitatively new effects compared to the equilibrium situations.[32] A dry big particle, driven in a subcritical liquid of small particles, becomes anisotropically dressed up with the small particles. The medium of the small particles shows an initial elastic response, followed by a long time diffusion regime, which is reflected in the drag force on a big particle moving through the small particles. The effective force between two driven dry particles in a subcritical liquid shows a deep minimum around the cross over of the two mechanisms of the medium response. Our observations can be verified by optical tweezer experiments on colloidal dispersions.[17] The occurrence of the deep minimum in the effective force between the dry spheres suggests applications in separation processes in macromolecular dispersions.

The importance of hydrodynamic interactions has been discussed for various solvent geometries relevant to our model system. Although for a variety of typical experimental setups, hydrodynamic interactions can be ignored, they become relevant for an unbounded solvent and neutral driven big particles. Then, the wake area of the driven large particle will be repopulated with more small particles at larger time. However, this should not at least qualitatively affect the cross over between the elastic and viscous regimes, arising out of the time scale separation of the motions of the two kinds of particles. Only the cross-over point may be shifted by the more efficient repopulation of the wake area. Clearly, this situation deserves more future studies using more sophisticated simulation schemes, such as the BD simulations with the Rotne–Prager mobility tensor[33] and stochastic rotation dynamics,[34] recently applied for colloids driven in a gravitational field.

ACKNOWLEDGMENTS

[1] S. Dietrich, in *Phase Transitions and Critical Phenomena*, edited by C. Domb and J. L. Lebowitz (Academic, London, 1988), Vol. 12, pp. 1–128.
[2] C. Bauer, T. Bieker, and S. Dietrich, Phys. Rev. E **62**, 5324 (2000).
[3] S. Herminghaus, Adv. Phys. **54**, 221 (2005).
[4] A. Fingerle and S. Herminghaus, Phys. Rev. Lett. **97**, 078001 (2006).
[5] D. Beysens and D. Esteve, Phys. Rev. Lett. **54**, 2123 (1985).
[6] T. Araki and H. Tanaka, Phys. Rev. E **73**, 061506 (2006).
[7] L. R. Snyder and J. J. Kirkland, *Introduction to Modern Liquid Chromatography* (Wiley, New York, 1979).
[8] P. A. Mourier, E. Eliot, M. H. Caude, R. H. Rosset, and A. G. Tambute, Anal. Chem. **57**, 2819 (1985); S. B. Hawthorne, C. B. Gabranski, E. Martin, and D. J. Miller, J. Chromatogr., A **892**, 421 (2000).
[9] K. Lum, D. Chandler, and J. D. Weeks, J. Phys. Chem. B **103**, 4570 (1999).
[10] J. Dzubiella, J. M. J. Swanson, and J. A. McCammon, Phys. Rev. Lett. **96**, 087802 (2006).
[11] J. Chakrabarti, S. Chakrabarti, and H. Loewen, J. Phys.: Condens. Matter **18**, L81 (2006).
[12] C. Bechinger, D. Rudhardt, P. Leiderer, R. Roth, and S. Dietrich, Phys. Rev. Lett. **83**, 3960 (1999).
[13] A. A. Louis, E. Allahyarov, H. Löwen, and R. Roth, Phys. Rev. E **65**, 061407 (2002).
[14] S. Karanikas and A. A. Louis, Phys. Rev. Lett. **93**, 248303 (2004).
[15] J. Liu and E. Luijten, Phys. Rev. Lett. **93**, 247802 (2004).
[16] G. A. Vliegenthart and P. van der Schoot, Europhys. Lett. **62**, 600 (2003).
[17] M. Köppl, P. Henseler, A. Erbe, P. Nielaba, and P. Leiderer, Phys. Rev. Lett. **97**, 208302 (2006).
[18] C. Reichhardt and C. J. O. Reichhardt, Phys. Rev. Lett. **96**, 028301 (2006).
[19] M. P. Allen and D. J. Tildesley, *Computer Simulation of Liquids* (Oxford University Press, New York, 1987).
[20] J. Chakrabarti, J. Dzubiella, and H. Loewen, Europhys. Lett. **61**, 415 (2003).
[21] R. Biswas and J. Chakrabarti, J. Phys. Chem. B **111**, 13743 (2007).
[22] J.-P. Hansen and A. R. McDonald, *Theory of Simple Liquids* (Academic, London, 1986).
[23] J. Dzubiella, H. Löwen, and C. N. Likos, Phys. Rev. Lett. **91**, 248301 (2003).
[24] E. Guyon, J.-P. Hulin, L. Petit, and C. D. Mitescu, *Physical Hydrodynamics* (Oxford University Press, Oxford, 2001).
[25] D. Long and A. Ajdari, Eur. Phys. J. E **4**, 29 (2001).
[26] M. Rex and H. Löwen, Eur. Phys. J. E **26**, 143 (2008).
[27] J. M. Victor and J. P. Hansen, J. Chem. Soc., Faraday Trans. 2 **81**, 43 (1985).
[28] B. Cui, H. Diamant, B. Lin, and S. A. Rice, Phys. Rev. Lett. **92**, 258301 (2004).
[29] A. Alvarez and R. Soto, Phys. Fluids **17**, 093103 (2005).
[30] E. R. Dufresne, T. M. Squires, M. P. Brenner, and D. G. Grier, Phys. Rev. Lett. **85**, 3317 (2000).
[31] O. B. Usta, A. J. C. Ladd, and J. E. Butler, J. Chem. Phys. **122**, 094902 (2005).
[32] BD simulations on an equilibrated wet big sphere in a subcritical gas of small particles shows that the small particles get stripped off the big sphere when the big sphere is driven strongly. The effective solvent mediated interaction between two such big spheres vanishes. The conclusions do not change even if the inertial term is added to the equations of motion (Ref. 22).
[33] M. Kollmann, R. Hund, B. Rinn, G. Nägele, K. Zahn, H. König, G. Maret, R. Klein, and J. K. G. Dhont, Europhys. Lett. **58**, 919 (2002).
[34] J. T. Padding and A. A. Louis, Phys. Rev. E **77**, 011402 (2008).